Magazine of Civil Engineering

ISSN 2712-8172

journal homepage: http://engstroy.spbstu.ru/

DOI: 10.34910/MCE.103.6

Mechanical safety of reinforced concrete frames under complex emergency actions

A.V. Alekseytsev
National Research Moscow State Civil Engineering University, Moscow, Russia
E-mail: aalexw@mail.ru

Keywords: reinforced concrete, dynamic behaviour, impact loading, column removal, progressive collapse, risk, safety, frames, nonlinear analysis

Abstract. An approach to the calculation of the frame reinforced concrete structures taking into account the potential risk of financial losses in an emergency is proposed. The simplified conditions for the strength of structural components considering the potential relative risk of the financial losses for the structure during emergency failure of these components is formulated. The strain-stress state analysis using the finite element method based on bar models can be performed in dynamics. The reinforced concrete structural component in the form of a package of concrete and reinforcement layers that can be deformed according to actual diagrams approximated by piecewise linear functions. The calculations were considered by accounting geometric, structural and physical nonlinearity. As an example, illustrating the operability of the presented approach, were considered the frame of the building with several scenarios for emergency actions. This is a complete or partial exclusion of one column from the calculation model, accompanied by a horizontal impact. The exclusion of 0.75 and 0.5 parts of the cross section of the column as well as its complete exclusion, accompanied by a horizontal impact pulse were examined. A collision of a damaged structure with a rigid barrier and with a deformable base were simulated. The proposed approaches to modeling the stress-strain state and strength conditions of the bar reinforced concrete systems have prospects for using in algorithms of optimum parametric synthesis of structures based on metaheuristic approaches.

1. Introduction

The safety of frame reinforced concrete structures of civil buildings and structures under mechanical emergency actions is investigated. To assess the stress-strain state, structural dynamics analysis is used taking into account physical, geometric and structural nonlinearities. In addition, the risk of local damage is taken into account.

In relation to the safety issue, many studies are devoted to the design of structures taking into account resistance to progressive collapse [1–3]. Many researchers considered the objective of ensuring the mechanical safety of building structures, in this case they studied the stability of the load-bearing structure to damages, including as a result of the impacts [4–10]. They examined the processes of deformation of a damaged system as well as the preservation of its geometrical invariability. At the same time, the sustainability (survivability) of the system should be ensured for the time necessary for the evacuation of people or equipment, and the shape of the deformed system should allow performing the evacuation. The most frequent local damage was the rapid removal of one of the column supports or pillars of the structure [11–14, 45]. One of the important objectives to be solved when assessing both the safety and the economic efficiency of the structural system is to take into account the nature of local damage that occurs during man-made actions and natural-climatic effects on operating buildings [15–17]. In most studies, in case of structural damage support bracing or columns is completely removed [18–20]. The force effect that caused the damage is also practically not considered. In fact, during structure failures, a case of collision of a damaged structure with a barrier often occurs. However, some of these barriers may collapse, and some may not. A characteristic case is a partial putting out of operation of the supporting component. Some illustrations of such failures are shown in Fig. 1.

Alekseytsev, A.V. Mechanical safety of reinforced concrete frames under complex emergency actions. Magazine of Civil Engineering. 2021. 103(3). Article No. 10306. DOI: 10.34910/MCE.103.6

Figure 1. Emergency actions on structures: a) impact with preservation of static force after action; b) local damage with partial exclusion of the pillar from work; c) the complete exclusion of the column, followed by the interaction of the structure with the deformable barrier; d) local damage without removing of the element.

In a number of works, experimental and theoretical studies were carried out in which a single local damage was considered in different parts of the structure. However, depending on the required level of structural safety, it may be necessary to take into account two, and three or more local damages [21–23]. Moreover, their occurrence may be dependent or independent of each other. Consideration of all these factors can significantly adjust the design results. As a rule, local structural damage that causes localized or progressive destruction is associated with socio-economic losses. At the same time, when calculating and optimizing structures, it is necessary to take into account reasonable safety factors [24, 25]. As a result of excessive resource saving, a less reliable and safe design can be obtained, the failure of which will cause large losses, that, in our opinion, is unacceptable. Therefore, along with the assessment of the conditions of strength, stiffness and stability for structures with a higher level of safety, it is necessary to apply criteria related to the risk assessment of such systems [26–30] and optimization of their parameters [31, 32]. One of the common types of load-bearing structures affected by loads not provided for normal operation are reinforced concrete frames and floor and roof slabs [33–35]. These structures in case of mechanical, high temperature and corrosion damage were studied.

Modern methods for calculating the load-bearing structures of buildings involve checking the requirements for the ultimate limit states. These requirements comprise satisfying inequalities such as $F<F_{ult}$, $f<f_{ult}$, etc. [36–40], where F, f are the calculated values of the force, deflection, etc., and F_{ult}, f are the limit values these variables, corresponding to the normal operation of the facility. Such an approach is described in regulatory documents; however, current socio-economic conditions show that this approach to design does not always ensure mechanical safety of structures. Therefore, improving methods for analyzing the stress-strain state and methods for assessing risks in the design of reinforced concrete structures is now especially important. The issue of modeling deformations of reinforced concrete frame structures during emergency under complex design conditions is also relevant. The proposed calculation models can be used both for optimum [41] and for traditional design of load-bearing structures for civil buildings [42, 43].

The purpose of research is to ensure the mechanical safety of reinforced concrete frame structures in complex emergency actions. This involves solving the following main tasks:

- the development of an approach to modeling deformations of structural systems with incomplete removal from load scheme of a damaged element, as well as taking into account the presence of barriers and interaction with them;
- taking into account local damage in the presence of a horizontal shock load, as well as in the presence of a foundation on deformable soil;
- the proposal to take into account the risks of the socio-economic consequences of an emergency.

2. Methods

2.1. Operation conditions for the load-bearing structures of buildings with an increased level of social responsibility

2.1.1. Strength conditions

The constraints of strength to ensure the mechanical safety of buildings and structures is formulated, accidents in which can lead to serious social consequences as well as for facilities that are strategically important for the development of the state. Analysis of numerous accidents and disasters associated with the destruction of buildings and structures has showed that progressive collapse is unacceptable for the facilities under consideration. According to this, we introduce the assumption that destruction in such facilities can lead to financial loss equal to n-times cost of the destroyed structure. Then the condition for ensuring the strength of structural systems can be written as follows:

$$\left(\frac{|\Omega|}{\Omega_{ult}} - r\right) \le 1;\ r = \frac{pU}{C}. \tag{1}$$

Where Ω is the internal force factor characterizing the mechanical stresses of the structure material; Ω_{ult} is the calculated (limit) value of Ω, r is the relative risk associated with the emergency, provided that it has occurred with probability p; C is the cost of the damaged structure, U is the amount of financial loss (cost) associated with damage to the other structures within the localization area of destruction.

In the formula (1) in a particular case, for example, for calculating steel structures, the value of the equivalent stress according to Mises maximum-strain-energy of failure can be taken as Ω, and the value of the design steel resistance can be taken as Ω_{ult}. Similarly, to calculate reinforced concrete structures, for example, according to normal sections under bending or sloping sections under the action of a transverse force, we can write:

$$\left(\frac{|M|}{M_{ult}} - r\right) \le 1; \quad \left(\frac{|Q|}{Q_b + Q_{sw}} - r\right) \le 1; \tag{2}$$

where M, Q are the internal forces in cross section; M_{ult} is the ultimate moment perceived by reinforced concrete section; Q_b, Q_{sw} are transverse (shear) forces perceived by concrete and reinforcement.

2.1.2. Deflection conditions

When assessing the stiffness of structures, first of all it means their ability not to show unacceptably large changes in geometry, determined by deflection $[f]$. In this case, even with local affecting adversely the strength of individual components, the condition of resistance to structural failure must be fulfilled. These changes in geometry should provide the ability to evacuate people and equipment from the building. As an example, we write the deflection condition for a multistoried building having floor-to-floor heights of 3 m and 4.2 m as follows:

$$f \le [f] = \begin{cases} 0.3H, & (2.5 \le \mathrm{H} \le 3.2) \\ 0.5H, & (3.2 < \mathrm{H} \le 4.6), \\ l/30, & l \ge 12 \end{cases} \tag{3}$$

where f, H, l (m) is the deflection of the structure the height of the floor and the span of the damages structure, respectively.

2.1.3. Buckling condition

The stability condition is formulated, similar to the strength condition, as an inequation into which the relative risk value is introduced to increase the structural stability margin:

$$\left(\frac{n}{n_{ult}} - r\right) \le 1; \tag{4}$$

where n, n_{ult} are the actual and limiting factors of buckling margin, respectively.

The probability of failure p during action associated with the occurrence of an emergency for facilities of industrial and civil construction is recommended to be taken in the range of 0.01–0.05. If the object belongs to the strategic military infrastructure facilities, then this probability can be increased to 0.5. It should be noted that for buildings not related to objects of strategic and social importance, the risk r cannot be taken into account, since the probability of failure for the structure, considering only its normal operation in such buildings, is (10^{-5}–10^{-7}), then $r \to 0$.

2.2. Finite-element modeling of local damage for engineering calculations and optimization algorithms in accidental situation

2.2.1. Formulation of structural analysis problems

In course of many studies of structural resistance to the progressive collapse during accidental exposures we have considered the quick removal of support bracing for one of the columns from the calculation model. In this case, the reason for this removal and the further interaction of the damaged and undamaged structure are hardly considered. Local damage is often examined without regard to the presence of a deformable ground. Let us consider the following simplified techniques for modeling the interaction of a damaged structure within the finite-element method:

- the complete exclusion of the element from the calculation model with a horizontal impact;
- the partial exclusion of the element from the calculation model with a horizontal impact;
- contact interaction of a damaged structure with an indestructible barrier;
- contact interaction of a damaged structure with a destructible barrier.

The modeling is performed for indicated types of local damages with finite element models using the bar elements with the possibility of taking into account structural-nonlinear behavior. We will perform the stress-strain analysis of the structure in dynamics based on numerical integration of the differential equation system for displacements of the damaged system, taking into account the simplified Rayleigh damping calculation model:

$$[M]\left(\alpha \dot{y}(t) + \ddot{y}(t)\right) + [K]\left(\beta \dot{y}(t) + y(t)\right) = F(t) + G\chi(t);\ \chi(t) = \begin{cases} 0, t < t_0 \\ 1, t \geq t_0 \end{cases}, \quad (5)$$

where $[M], [K]$ are the global matrices of mass and stiffness of the finite element model, respectively; $\ddot{y}(t)$, $\dot{y}(t)$, $y(t)$ are the vectors of accelerations, velocities and nodal displacements, respectively; $F(t)$ is the vector of the external load reduced to the nodes, G is the vector of impactor gravity forces, $\chi(t)$ is the Heaviside function, t_0 is the time moment after which the gravity should be taken into account, G; α, β are inertial and structural damping ratios. The case is considered when $\alpha = 0$, the coefficient $\beta = 0.04 - 0.07$. The Newmark recurrence scheme is used.

2.2.2. The model of deformations with the complete exclusion of an element with a horizontal impact

The support model is shown in Fig. 2.

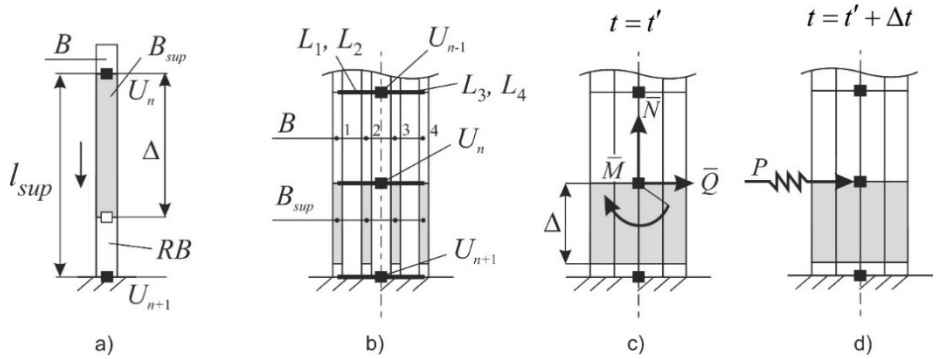

Figure 2. Modeling the support exclusion during emergency exposure: contact element (a); column support modelling (b); static equilibrium before emergency action (c); horizontal impact modelling (d).

Here, the elements $L_1 - L_4$ are rigid beams that define the eccentricities of the longitudinal axes of the bar elements B relative to the nodes U. Time moment t' is the point in time after which the the static equivalents of internal forces removing and applying the shock effect to the structure.

Let us introduce a spatial bar finite element B_{sup} having a length l_{sup}, between nodes U_n, U_{n+1}, while one of the nodes must be fixed against displacements, and the other connected to the spatial rod B, modeling the structure (Fig. 2, a). It is provided for possibility to set the gap Δ, modeled by low stiffness. The value of this gap should be calculated based on the accepted height of the column section, which is removed from operation. When the formal task is started, deformation by the size of the gap occurs, and then deformation begins on the fragment of the bar RB, which may have stiffness, simulating a solid object or an elastic-plastic deformable soil base. Modeling the complete exclusion of the support is performed in the following sequence:

- the static equivalents attached of internal forces to the node U_n, in the general case $\bar{M}, \bar{Q}, \bar{N}$, of equal to the support reactions. When calculating in dynamics, these forces are considered suddenly applied;
- the dynamic calculation begins in the time interval $[0; t']$, where t' is the time moment of dynamic relaxation, that is, the time during which the oscillations of the system with applied static equivalents $\bar{M}, \bar{Q}, \bar{N}$ are completely damped (Fig. 2, c);
- at the next moment of time $t' + \Delta t$ the forces $\bar{M}, \bar{Q}, \bar{N}$ are assumed to be zero, and in the same node a horizontal impact force appears, which is defined as $P = mkG$, where m is the mass of the impactor, kG is the mass acceleration, m, k is the specified coefficient, G is the gravity acceleration. Formalization of the presence and absence of these forces is carried out by determining the functions shown in Fig. 3.

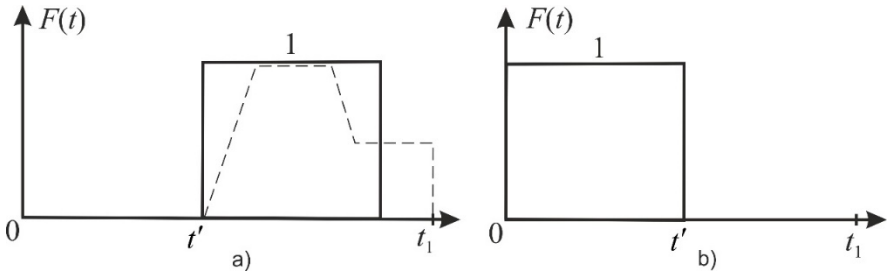

Figure 3. Functions for force P (a) and forces $\bar{M}, \bar{Q}, \bar{N}$ (b).

The dotted line in Fig. 3 shows a possible graph form for an impact pulse, a part of which is preserved after the maximum impact. Modeling of such a process corresponds to the action shown in Fig. 1, a.

2.2.3. Deformation model with partial exclusion of an element cross-section with a horizontal impact

To exclude support partially in case of local damage between nodes U_n, U_{n+1} it is introduced several elements on rigid consoles. In Fig. 2, four elements with consoles $L_1 - L_4$ are shown. For example, with the introduction of four elements of the same rigidity, it is possible to simulate the exclusion of 0.25 part of the section, if three elements B and one extreme element B_{sup} are introduced between the nodes under consideration. Accordingly, by increasing the number of elements B_{sup}, it is possible to simulate the exclusion of 0.5 and 0.75 parts of the section.

2.2.4. Contact interaction of a damaged structure with an indestructible barrier

The deformation model is described by the diagram shown in Fig. 4, c. This diagram is set for the final element B_{sup}, while the structural element "column" has a damaged section of length $l_{dam} = \varepsilon_0 l_{\text{sup}}$, (Fig. 4 a, c).

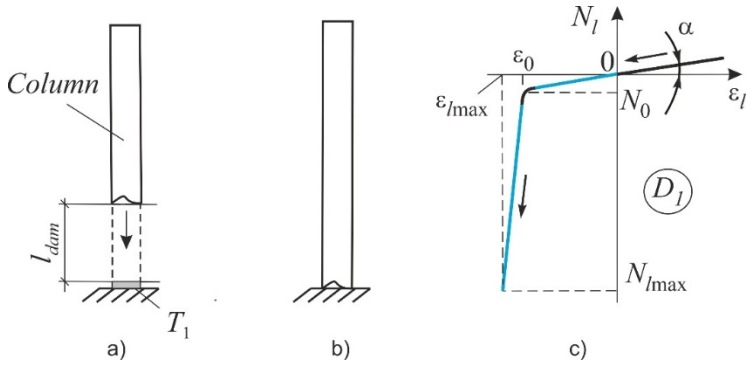

Figure 4. Modeling interaction with an indestructible barrier: the column exists before contact interaction with the barrier (a); the column is present after this interaction (b) the contact modeling diagram (c).

The segment of the diagram, limited by points $(\varepsilon_0; N_0)$ and $(\varepsilon_{l\max}; N_{l\max})$ determines the presence of a barrier T_1, which at large values $N_{l\max}$ can be approximately considered rigid. The deformations of the bar in this section correspond to the situation shown in Fig. 4, b. The parameter α in the diagram is a small number that ensures the stability of the numerical integration procedure; this parameter is the angle in radians varies between 0.01–0.1 depending on the type of chart.

At the point $(\varepsilon_0; N_0)$, the diagram has a rounding, which is also necessary to ensure the stability of the dynamic analysis procedure, where ε_0 is fictitious relative deformations of the contact element corresponding to the size of the damaged part of the rod that is loss. The Value N_0 is a fictitious small value of the longitudinal force, set equal to 10-100 N, which can be interpreted as the conditional resistance of the environment during deformation from the moment of local damage to contact interaction with the barrier.

Values $\varepsilon_{l\max}; N_{l\max}$ are relative deformation and longitudinal force arising from contact with an infinitely rigid barrier. In each computing process, these parameters are selected individually, but as the initial approximation for calculating frame structures, you can specify $\varepsilon_{l\max} \approx 1.02\varepsilon_0; N_{l\max} \approx 10^3 - 10^4 R_{\max}$, where $R_{\max}$ is the module of the maximum vertical support reaction for the calculated system.

2.2.5. Contact interaction of a damaged structure with a destructible barrier

The deformation process consists of the following stages:

- collision with a deformable barrier T_2. In this case, the final element has absolute shortening Δl_{01} (Fig. 5, a) at the value N_0 of the longitudinal force (segment 0;0 – $(\varepsilon_{01}; N_0)$ in the diagram of Fig. 5, d), which corresponds to the position of the structure in Fig. 5, b;
- deformation of the barrier T_2. The segment with the projection of its relative deformation determines the load-bearing capacity of this barrier ε_{br}. In this case, the ultimate longitudinal force that the barrier can withstand is equal N_{br}.
- destruction of the barrier and displacement before contact with the barrier T_1. In this case, the bar has relative shortening Δl_{02}, which corresponds to a length segment ε_{02}. Distances δ are fictitious small relative deformations that ensure the stability of the process of numerical integration. The last linear section of the diagram simulates the stiffness of the barrier T_1, considered rigid. The final position of the bar corresponds to Fig. 5, c.

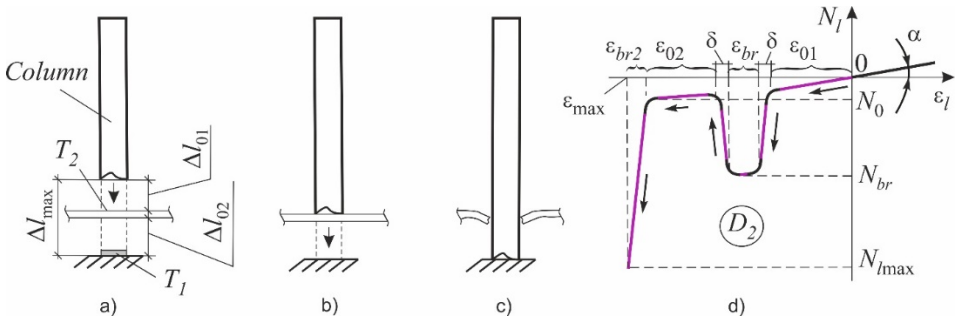

Figure 5. Modeling the interaction with destructible and indestructible barriers: structure after their part removing (a), T_1, T_2 – marks of the barriers; stages of interaction (b), (c); chart of modelling the barrier T_2 destruction; D_2 – diagram labeling.

The α parameter is the same as in Fig. 4. The maximum deformations $\varepsilon_{\max}$ of the contact element (Fig. 5) are the sum of: $\varepsilon_{\max} = 2\delta + \varepsilon_{01} + \varepsilon_{02} + \varepsilon_{br} + \varepsilon_{br2}$. The value ε_{br2} is the infinitesimal deformation of the barrier T_1. The value of the force N_0 is close to zero, it is approximately equal to the resistance of the environment on the segments Δl_{01} and Δl_{02}.

2.3. Finite-element modeling of reinforced concrete structures with local damage

2.3.1. Modeling damage that does not progress after local action

The deformation modeling the reinforced concrete beams is represented as a package of concrete layers C_b and reinforcing layers C_r (Fig. 6, a). In general, for the cross section, the Bernoulli hypothesis and the assumption that the layers do not exert pressure on each other are fulfilled. The implementation of such a model can be carried out by constructing a stiffness matrix for the element, taking into account the fact that each layer can have tension-compression strains. To modeling the deformations of reinforced concrete columns, parts of which can be excluded in the calculation process, another model is used (Fig. 6, b).

The cross-section is divided into parts 1-4, presented in the form of separate bars with common nodes. The position of these bars is determined by the length of the consoles defined by the projections y_b, z_b, y_r, z_r in the local axes of the element. For those elements that will be partially or fully susceptible to local damage, it may be possible to be operated according to the diagram D_1 (Fig. 4, c).

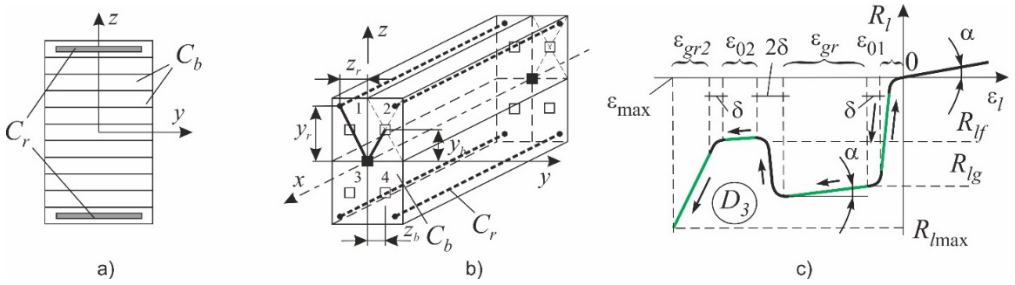

Figure 6. Modeling of deformation of reinforced concrete beams (a), columns (b) and soil foundation (c).

A simplified diagram of the deformation of the soil base (Fig. 6, c) can be described using the following sections. The first is determined by the point $(\varepsilon_{01}; R_{lg})$, ε_{01} where are the relative elastic deformations of the soil, R_{lg} is the calculated resistance to compression of the soil base. Further, the soil is deformed plastically and receives deformations ε_{gr}. The site corresponding to the level R_{lf} of stresses in the soil and deformations ε_{02} models the fail of the soil base associated with the loss of bearing capacity. This can happen if there are fluid lenses, karst cavities, etc. in the ground. Deformation $\varepsilon_{\max}$ here simulate the presence of incompressible soil, $\varepsilon_{\max} = 4\delta + \varepsilon_{01} + \varepsilon_{02} + \varepsilon_{gr} + \varepsilon_{gr2}$.

For the remaining elements, deformation diagrams are set that correspond to the operation of concrete and reinforcement under load. These diagrams for reinforcement and concrete, respectively, are presented in Fig. 7, a,b. The lines shown in black on these diagrams are introduced to ensure the stability of the process of numerical integration of equations (5). The magnitude of the forces and deformations $N_{s0}, \varepsilon_{s0}, \varepsilon_{s1}, N_{b1}, \varepsilon_{b1}, \varepsilon_{b2}, N_{bt}, \varepsilon_{bt}$ are determined depending on the class of concrete and reinforcement approved in the design of the structure. Fig. 7, c-f shows the model of the supporting part of the reinforced concrete column when considering the possibility of destruction 0.25, 0.5 and 0.75 parts of the concrete section. In each of these cases, an operation diagram D_1 is introduced for the one element or several elements to be excluded (Fig. 4).

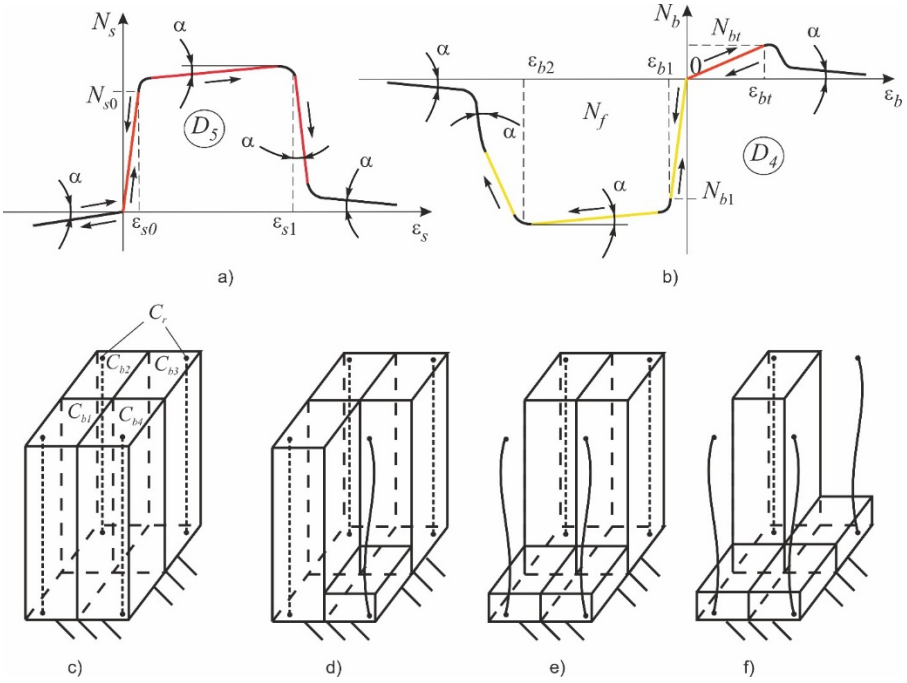

Figure 7. Diagrams of deformation of steel (a) and concrete (b) and a model of partial damage to the column: without damages (c), damage of a quarter (d), half (e) and three quarters (f) of column segment.

2.3.2. Progressive local damages

The structure of concrete makes it possible for propagating local damages to occur both during and after emergency action. These effects can be approximately modeled by dynamic calculations of damaged systems, taking into account structural nonlinearity in the operation of a part of the cross-section exposed to local effects. One of the common cases of such effects is mechanical damage to the column, for example, in a collision with a car or other moving deformable object. In the case of an angular collision (Fig. 8, a) or a frontal impact (Fig. 8, b), it is possible to approximately model the progressive collapse of the parts of the column that are shaded in gray. In a more general case, for example, with accumulated defects as a result of long-term operation, a local impact can initiate the exclusion of the outer layers of the column while maintaining the operability of the inner core (Fig. 8, c, Fig. 1, b). Modeling the exclusion of a cross section quarter from a concrete column in time will be shown using the example of Fig. 8, d, e. The cross section of the column is modeled by seven beam elements. Three of them, the cross sections of which are shown by squares without filling, are modeled by ordinary spatial bars, for which the operation diagram D_4 is provided. Bars with cross-sections 1-4 (Fig. 8, d) are contact elements that operate according to the diagram D_1. Initially, these elements are balanced by the static equivalents of the reactions $\bar{N}_1 - \bar{N}_4$, perceived by the quarter section. All these forces act during the relaxation time $[0;t']$. Then the force $\bar{N}_1$, acting over time $[t';t'_1]$ is permanently equal to zero and does not act within the time interval $(t'_1;t_1]$ (Fig. 8, e). The remaining forces $\bar{N}_2 - \bar{N}_4$ continue to operate. The time $[t'_1;t'_2]$ can be short, which approximately corresponds to the propagation time of local damage in the material. Further, the force $\bar{N}_2$ at time moment t'_2 is removed similarly to the force $\bar{N}_1$. The process is repeated until the exclusion of

force $\overline{N}_4$. By the same scheme, it is possible to simulate the exclusion of any parts of the cross sections under various influences, for example, during impacts shown in Fig. 8, a, b.

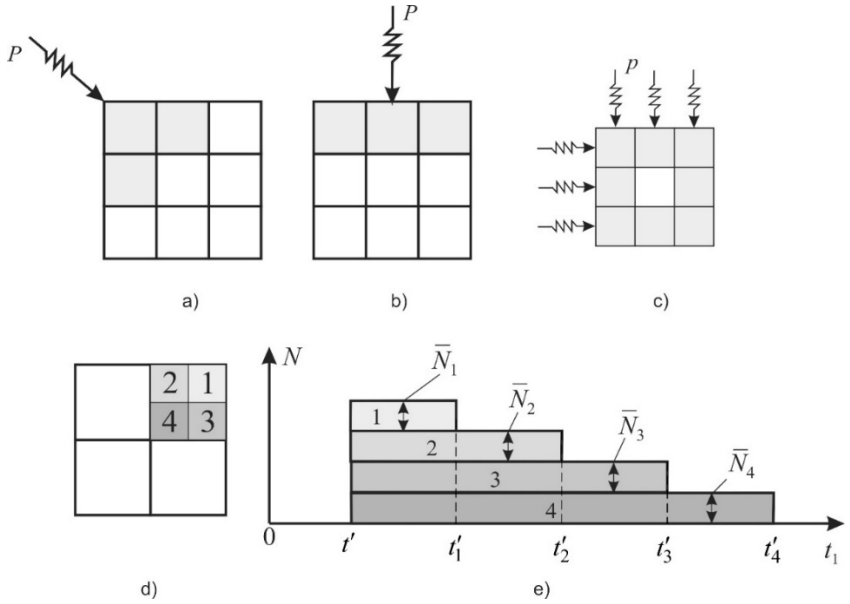

Figure 8. Modeling the exclusion of part of the cross sections of bar elements: (a)-(c) variants of emergency actions and damages volumes; sequence of emergency destruction the cross section material (d); time history of emergency action process (e).

The process of deformations propagation after local damage for reinforced concrete sections is a very difficult phenomenon for modeling, which depends on the type of emergency action, on the pre-emergency loading of the section, on the structure and percent of concrete reinforcement. According to many studies, the rate of deformations during impacts for concrete structures of columns varies within wide limits $\dot{\varepsilon} = 10^{-6} \div 10^{2}$ 1/sec, and the time of destruction of sections $\tilde{t}_d = 0.5 - 14$ ms. Initially, on the basis of experimental data or numerical simulation, the time t_d of complete exclusion of a part of the section from work is determined. With an equal area of the excluded elements, the intervals $t_1 - t_4$ are approximately equal:

$$t_1[t'_1; t'] = t_2[t'_2; t'_1] = t_3[t'_3; t'_2] = t_4[t'_4; t'_3] = t_d / 4 \tag{6}$$

With an unequal area, the size of the intervals is determined by the formula:

$$t_d = \frac{s_1}{s_d} t_1[t'_1; t'] + \frac{s_2}{s_d} t_2[t'_2; t'_1] + \frac{s_3}{s_d} t_3[t'_3; t'_2] + \frac{s_4}{s_d} t_4[t'_4; t'_3], \tag{7}$$

where $s_1 - s_4$ are the areas of elements 1-4 on Fig. 8., s_d is the area of the entire part of the excluded section.

3. Results and Discussion

3.1. Description of the object calculation model

The reinforced concrete frame of the building is considered, shown in Fig. 9. Three design cases are considered:

- *Case 1. "Calculation of a plane frame on a foundation slab (interaction with an indestructible barrier)"*. We performed the support exclusion modeling using the diagram B1 on Fig. 9. At the same time, the parameters of the GAP element provided a gap of 15 cm, after which the system interacted with the element having stiffness exceeding 1,000 times stiffness of the column. The gap is assigned on the condition that it should be less than the length of the contact element, that is, 0.5 m. Some results of dynamic analysis are presented in Fig. 11 a, c, d. The abscissa axis shows the calculation numbers corresponding to the integration step.

- *Case 2. "Calculation when excluding the support without contact interaction".* This calculation was performed according to the well-known scheme described in many papers, but taking into account the horizontal impact interaction. Some data on system displacements are shown in Fig. 11. b, d. Obviously, these oscillations of the system are abstract in nature. Fig. 11, d shows that the deflection of the crossbars during contact interaction (with the exception of a fragment of a structure measuring 15 cm) is less than during oscillations without contact constraints.
- *Case 3. "Calculation of the frame on an inelastic soil, taking into account the partial exclusion of the middle pillar".* The exclusion of 0.75 and 0.5 parts of the column section is modeled. We denote these scenarios as S1 and S2. Soil was taken in the form of clay with porosity ratio of 0.5 and index of liquidity as IL = 1. It was supposed that under each support there is a square foundation of 2.5 m wide with a depth of 2 m. Soil deformations are described by a diagram D_3 in Fig. 6, c at $R_{lf} = R_{lg}$ = 430 kPa. In case of removal of 0.75 part of the cross section, the remaining part of the section quickly collapsed. The time for excluding parts of the cross sections was taken equal: $t_{d,075}$ = 7.5 ms, $t_{d,05}$ = 5 ms. Fig. 13 shows some calculation results. With the exclusion of part of the column, significant displacements from the plane of the frame are observed, which is a sign of the need to take into account the survivability of the structure as a whole, considering its spatial deformation.

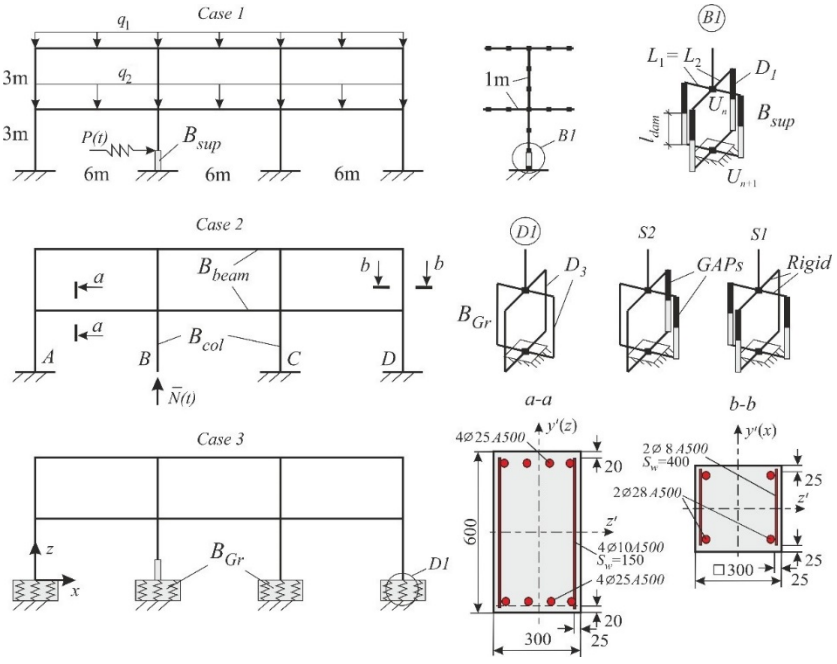

a) **b)**

Figure 9. An example of the calculation of a reinforced concrete frame: load scheme (a) and stress-strain state modelling (b); B_{beam}, B_{col} – finite element packages for rigel and column modelling shown in Fig. 6, a, b; B_{sup}, B_{Gr} – same packages for support and soil modelling.

The calculation was performed using the Femap software package with the NX Nastran solver. Module «Nonlinear Transient Response» is used. The integration step was selected automatically. It was assumed q_1 = 18 kN/m, q_2 = 24 kN/m, $P(t) = Pf_1(t)$, see Fig. 9, 10, a. The constraint force in the removed element changes $R(t) = R_{st}f_2(t)$, see Fig. 10, b. P = 80 kN, R_{st} is the reaction (axial forces, bending moments, shear forces) selected taking into account the static calculation. Concrete has design compression resistance of 25 MPa, tensile strength of 1.45 MPa. The reinforcement has design resistance of 450 MPa. Physically nonlinear operation on D_4, D_5 diagrams was taken into account for these materials. The transient nonlinear dynamic process had duration of 5 sec, after 2 sec, in event of the structure with the barrier interaction, the oscillations completely damped. If there was no contact interaction, the oscillations were observed for 4 sec. Therefore, the abscissa axis in Fig. 10 are limited to 4.1. The dynamic relaxation time after application of the load was taken to be 1 s. Overall structural damping with a ratio equal 0.05 was taken into account.

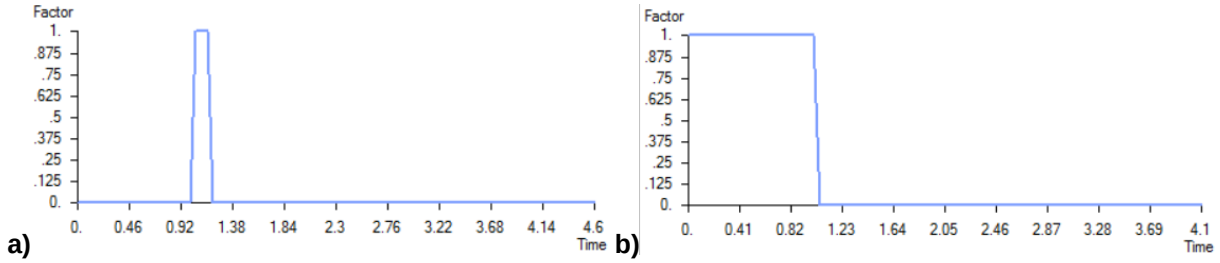

Figure 10. The form of the functions $f_1(t)$ (a) and $f_2(t)$ (b).

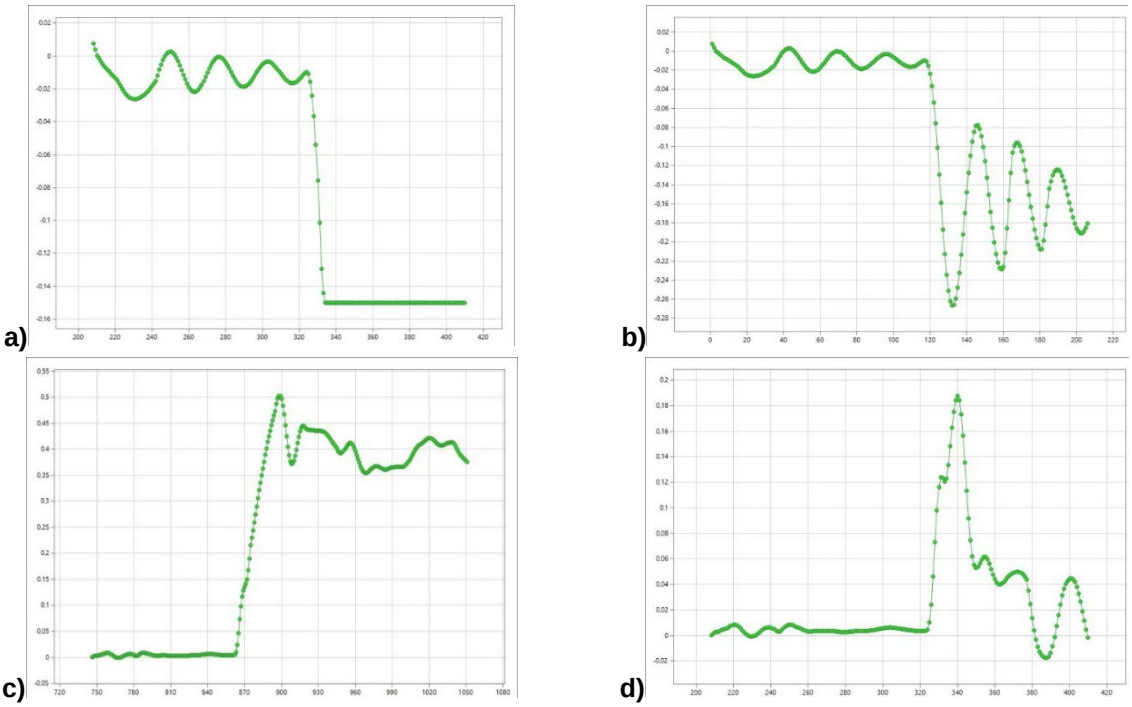

Figure 11. Dependence on the displacements in the time: a) vertical displacements of the damaged end part of the column upon impact with a barrier; b) the same without considering the contact interaction; c) horizontal movements when exposed to horizontal impact, taking into account contact interaction; d) the same, without contact interaction.

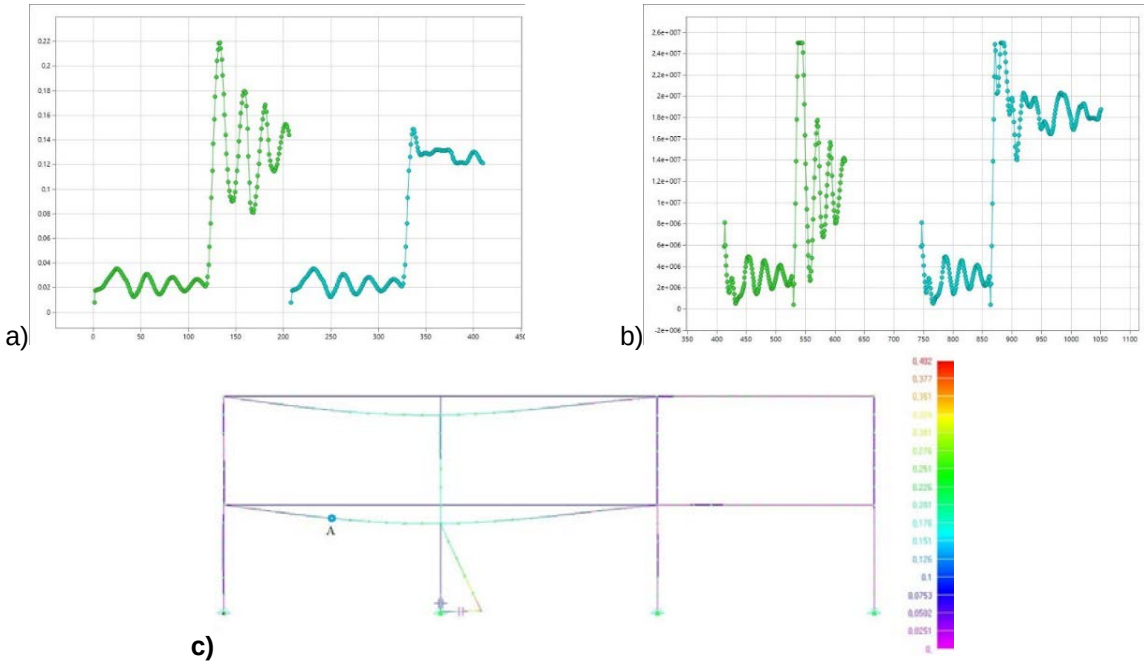

Figure 12. The calculation results: a) vertical displacements of the first floor beam at 3 m distance from the leftmost support (point A) without contact interaction (left) and with it (right); b) compression stress in concrete (in modulus) at point A; c) deformed frame layout after horizontal impact and taking into account contact interaction.

3.2. Example of calculating a structural component taking into account the risks of financial losses

As financial loss U in the formula (1), we take into account components in which deformations occur equal or close to ultimate fracture deformations. It is assumed that the probability of emergency action to be p = 0.8, which means that it will happen rather than not. Designing an intact middle column were performed. As a complete structure, only the frame in question were considered. During normal operation, the cross-sectional area is determined primarily by structural requirements, and the operational compression stresses in concrete are in modulus about 6 MPa, $\Omega = 6MPa$, $\Omega_{ult} = 25MPa$. In case of local destruction, including the Case 1 scenario, while ensuring survivability, beams of the 1st and 2nd floors in 2 spans and the middle column on each floor can fail. Then conditionally the damage can be calculated as the ratio of the lengths of the components $r = 0.8 \cdot 30 / 60 = 0.4$, $\Omega / \Omega_{ult} = 6/25 = 0.24$. Then, according to the formula (1): 0.24+0.4=0.64≤1, the condition is satisfied. That is, the approved structural solution for the column contains the necessary margin of safety to ensure survivability with an emergency action the probability of occurrence of which is 0.8. It should be noted that if the actual margin of safety for the column is less than 36 %: $\Omega / \Omega_{ult} \geq 0.64$, the column would lose strength or stability if the emergency scenario under consideration occurs.

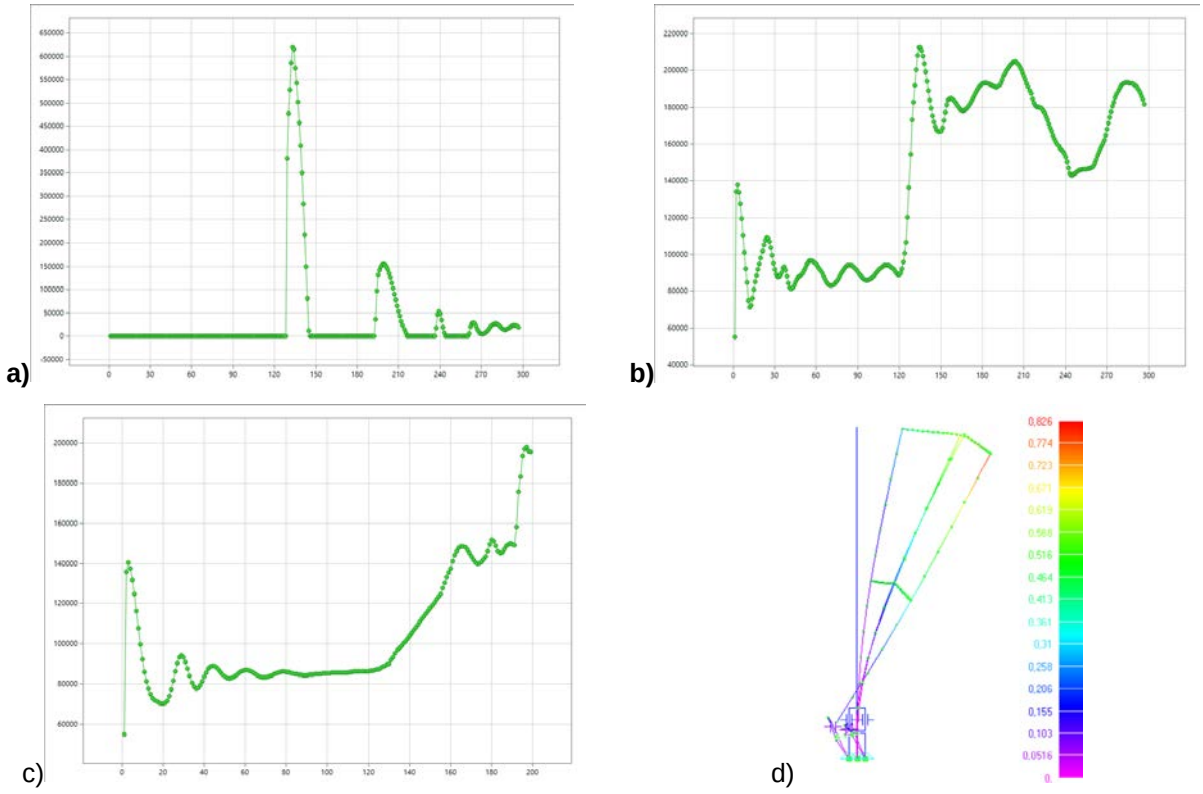

Figure 13. Results of the calculation with partial local damage: a) contact stresses during the interaction of the damaged column with the foundation; b) change in time of the compression stresses in the soil of the middle support (S1); c) the same, but under scenario (S2); d) total translations of the system (view from the plane of the frame)

3.3. Discussion

The proposed deformation modeling methods are simplified, but have an acceptable amount of computation for use in optimization algorithms, for example, [18, 26, 44]. It seems promising to use these models for an approximate assessment of the deformations of reinforced concrete structures under high-temperature effects [25] and a combination of mechanical damage and the action of temperature. Existing approaches to the rapid exclusion of column supports from the calculation model, which do not include consideration of the reasons for this exclusion (for example, horizontal impact, modeling a structure collision with barriers), can significantly distort the picture of the stress-strain state of these structures. In turn, this can affect the provision of mechanical safety in an emergency.

4. Conclusion

1. The methodology for the approximate calculation of the frame reinforced concrete load-bearing structures, which takes into account on equal terms the limiting conditions and risks of financial losses associated with the possible occurrence of an emergency were proposed. This approach can be used to optimize design solutions under constraints associated with the mechanical safety of facilities.

2. For calculation of the stress-strain state of reinforced concrete structures based on the finite element method the alternative simplified approaches were proposed which allow modeling a horizontal impact with the subsequent complete or partial exclusion of part of the concrete cross-section from operation, collision of the damaged structure with a destructible or non-destructible barrier, simplified interaction of the damaged structure with a soil foundation.

References

1. Kokot, S., Anthoine, A., Negro, P., Solomos, G. Static and dynamic analysis of a reinforced concrete flat slab frame building for progressive collapse. 2012. Engineering Structures. 40. Pp. 205–217. DOI: 10.1016/j.engstruct.2012.02.026
2. Serpik, I.N., Alekseytsev, A.V. Optimization of frame structures with possibility of emergency actions. 2013. Magazine of Civil Engineering. 44 (9). DOI: 10.5862/MCE.44.3
3. Qian, K., Zhang, X. De, Fu, F., Li, B. Progressive collapse-resisting mechanisms of planar prestressed concrete frame. 2019. ACI Structural Journal. 116 (4). Pp. 77–90. DOI: 10.14359/51715567
4. Baca, M., Rybak, J., Tamrazyan, A.G., Zyrek, T. in (2016) Int. Multidiscip. Sci. GeoConference Surv. Geol. Min. Ecol. Manag. SGEM. Pp. 945–950. DOI: 10.5593/SGEM2016/B11/S02.119
5. Chen, Y., May, I.M. Reinforced concrete members under drop-weight impacts. 2009. Proceedings of the Institution of Civil Engineers: Structures and Buildings. 162 (1). Pp. 45–56. DOI: 10.1680/stbu.2009.162.1.45
6. Chuzel-Marmot, Y., Ortiz, R., Combescure, A. Three dimensional SPH-FEM gluing for simulation of fast impacts on concrete slabs. 2011. Computers and Structures. 89 (23–24). Pp. 2484–2494. DOI: 10.1016/j.compstruc.2011.06.002
7. Del Linz, P., Fan, S.C., Lee, C.K. Modeling of combined impact and blast loading on reinforced concrete slabs. 2016. Latin American Journal of Solids and Structures. 13 (12). Pp. 2266–2282. DOI: 10.1590/1679-78252516
8. Gokkaya, B.U., Baker, J.W., Deierlein, G.G. Estimation and impacts of model parameter correlation for seismic performance assessment of reinforced concrete structures. 2017. Structural Safety. 69. Pp. 68–78. DOI: 10.1016/j.strusafe.2017.07.005
9. Leppänen, J. Dynamic behaviour of concrete structures subjected to blast and fragment impacts. 2002. … of Structural Engineering, Concrete Structures. Pp. 96. https://www.msb.se/Upload/Insats_och_beredskap/Olycka_kris/Skydds-rum/Litteratur/Akademiska avhandlingar/Dynamic Behaviour of Concrete Structures subjected to Blast and Fragment Impacts.pdf
10. Qasrawi, Y., Heffernan, P.J., Fam, A. Dynamic behaviour of concrete filled FRP tubes subjected to impact loading. 2015. Engineering Structures. 100. Pp. 212–225. DOI: 10.1016/j.engstruct.2015.06.012
11. Weng, J., Tan, K.H., Lee, C.K. Modeling progressive collapse of 2D reinforced concrete frames subject to column removal scenario. 2017. Engineering Structures. 141. Pp. 126–143. DOI: 10.1016/j.engstruct.2017.03.018
12. Yang, T., Han, Z., Deng, N., Chen, W. Collapse responses of concrete frames reinforced with BFRP bars in middle column removal scenario. 2019. Applied Sciences (Switzerland). 9 (20). DOI: 10.3390/app9204436
13. Tamrazyan, A., Alekseytsev, A. Evolutionary optimization of reinforced concrete beams, taking into account design reliability, safety and risks during the emergency loss of supports in (2019) E3S Web Conf. DOI: 10.1051/e3sconf/20199704005
14. Mistri, A., Sarkar, P., Davis, R. Column-beam moment capacity ratio and seismic risk of reinforced concrete frame building. 2019. Proceedings of the Institution of Civil Engineers: Structures and Buildings. 172 (3). Pp. 189–196. DOI: 10.1680/jst-bu.17.00100
15. Lazar Sinković, N., Dolšek, M. Fatality risk and its application to the seismic performance assessment of a building. 2020. Engineering Structures. 205. DOI: 10.1016/j.engstruct.2019.110108
16. Araya-Letelier, G., Parra, P.F., Lopez-Garcia, D., Garcia-Valdes, A., Candia, G., Lagos, R. Collapse risk assessment of a Chilean dual wall-frame reinforced concrete office building. 2019. Engineering Structures. 183. Pp. 770–779. DOI: 10.1016/j.engstruct.2019.01.006
17. Haselton, C.B., Liel, A.B., Deierlein, G.G., Dean, B.S., Chou, J.H. Seismic collapse safety of reinforced concrete buildings. I: Assessment of ductile moment frames. 2011. Journal of Structural Engineering. 137 (4). Pp. 481–491. DOI: 10.1061/(AS-CE)ST.1943-541X.0000318
18. Kabantsev, O.V., Tamrazian, A.G. Allowing for changes in the calculated scheme during the analysis of structural behaviour. 2014. Magazine of Civil Engineering. 49(5). Pp. 15–26; 123–124. DOI: 10.5862/MCE.49.2
19. Nguyen, W., Bandelt, M.J., Trono, W., Billington, S.L., Ostertag, C.P. Mechanics and failure characteristics of hybrid fiber-reinforced concrete (HyFRC) composites with longitudinal steel reinforcement. 2019. Engineering Structures. 183. Pp. 243–254. DOI: 10.1016/j.engstruct.2018.12.087
20. Tamrazyan, A., Avetisyan, L. in (2014) Appl. Mech. Mater. Pp. 62–65. DOI: 10.4028/www.scientific.net/AMM.638-640.62
21. Alekseytsev, A. V. in (2020) J. Phys. Conf. Ser. DOI: 10.1088/1742-6596/1425/1/012014
22. Prokurov, M., Indykin, A., Alekseytsev, A. in (2018) MATEC Web Conf. DOI: 10.1051/matecconf/201825104017
23. Terrenzi, M., Spacone, E., Camata, G. Collapse limit state definition for seismic assessment of code-conforming RC buildings. 2018. International Journal of Advanced Structural Engineering. 10 (3). Pp. 325–337. DOI: 10.1007/s40091-018-0200-6
24. Alekseytsev, A.V., Akhremenko, S.A. Evolutionary optimization of prestressed steel frames. 2018. Magazine of Civil Engineering. 81 (5). Pp. 32–42. DOI: 10.18720/MCE.81.4
25. Serpik, I.N., Alekseytsev, A.V., Balabin, P.Y., Kurchenko, N.S. Flat rod systems: Optimization with overall stability control. 2017. Magazine of Civil Engineering. 76 (8). Pp. 181–192. DOI: 10.18720/MCE.76.16
26. Shokrabadi, M., Burton, H.V. Risk-based assessment of aftershock and mainshock-aftershock seismic performance of reinforced concrete frames. 2018. Structural Safety. 73. Pp. 64–74. DOI: 10.1016/j.strusafe.2018.03.003

27. Sinković, N.L., Brozovič, M., Dolšek, M. Risk-based seismic design for collapse safety. 2016. Earthquake Engineering and Structural Dynamics. 45 (9). Pp. 1451–1471. DOI: 10.1002/eqe.2717
28. Xue, B., Le, J.L. in (2016) Am. Concr. Institute, ACI Spec. Publ. Pp. 105–121.
29. Yu, X., Lu, D., Li, B. Estimating uncertainty in limit state capacities for reinforced concrete frame structures through pushover analysis. 2016. Earthquake and Structures. 10 (1). Pp. 141–161. DOI: 10.12989/eas.2016.10.1.141
30. Nili, M., Ghorbankhani, A.H., Alavinia, A., Zolfaghari, M. Assessing the impact strength of steel fibre-reinforced concrete under quasi-static and high velocity dynamic impacts. 2016. Construction and Building Materials. 107. Pp. 264–271. DOI: 10.10-16/j.conbuildmat.2015.12.161
31. Alekseytsev, A.V. Evolutionary optimization of steel trusses with the nodal joints of rods. 2013. Magazine of Civil Engineering. 40 (5). Pp. 28–37. DOI: 10.5862/MCE.40.3
32. Ngo, T., Mendis, P. Modelling the dynamic response and failure modes of reinforced concrete structures subjected to blast and impact loading. 2009. Structural Engineering and Mechanics. 32 (2). Pp. 269–282. DOI: 10.12989/sem.2009.32.2.269
33. Kyriakides, N., Sohaib, A., Pilakoutas, K., Neocleous, K., Chrysostomou, C., Tantele, E., Votsis, R. Evaluation of Seismic Demand for Substandard Reinforced Concrete Structures. 2018. The Open Construction and Building Technology Journal. 12 (1). Pp. 9–33. DOI: 10.2174/1874836801812010009
34. Mastali, M., Ghasemi Naghibdehi, M., Naghipour, M., Rabiee, S.M. Experimental assessment of functionally graded reinforced concrete (FGRC) slabs under drop weight and projectile impacts. 2015. Construction and Building Materials. 95. Pp. 296–311. DOI: 10.1016/j.conbuildmat.2015.07.153
35. Magnusson, J., Hallgren, M., Ansell, A. Shear in concrete structures subjected to dynamic loads. 2014. Structural Concrete. 15 (1). Pp. 55–65. DOI: 10.1002/suco.201300040
36. Ismail, M., Mueller, C.T. Computational structural design and fabrication of hollow-core concrete beams. 2018. Proceedings of the IASS Symposium 2018.
37. Mansur, M.A., Tan, K.-H., Weng, W. Analysis of Reinforced Concrete Beams with Circular Openings Using Strut-and-Tie Model. 2001. Structural Engineering, Mechanics and Computation. Pp. 311–318. DOI: 10.1016/b978-008043948-8/50030-8
38. Niroomandi, A., Pampanin, S., Dhakal, R.P., Ashtiani, M.S., De La Torre, C. Rectangular RC walls under bi-directional loading: recent experimental and numerical findings. 2018. The Concrete NZ Conference 2018.
39. Abed, F., Alhafiz, A.R. in (2018) 2018 Adv. Sci. Eng. Technol. Int. Conf. ASET 2018. Pp. 1–5. DOI: 10.1109/ICASET.20-18.8376768
40. Zeng, X. Finite Element Analysis of Square RC Columns Confined by Different Configurations of Transverse Reinforcement. 2017. The Open Civil Engineering Journal. 11 (1). Pp. 292–302. DOI: 10.2174/1874149501711010292
41. Alekseytsev, A.V., Al Ali, M. Optimization of hybrid I-beams using modified particle swarm method. 2018. Magazine of Civil Engineering. 83 (7). Pp. 175–185. DOI: 10.18720/MCE.83.16
42. Ranade, R., Li, V.C., Heard, W.F., Williams, B.A. Impact resistance of high strength-high ductility concrete. 2017. Cement and Concrete Research. 98. Pp. 24–35.
43. Pontiroli, C., Arlery, M., Rouquand, A. in (2015) Response Struct. Under Extrem. Load. Pp. 523–529.
44. Alekseytsev, A.V., Gaile L., Drukis, P. Optimization of steel beam structures for frame buildings subject to their safety requirements. Magazine of Civil Engineering. 2019. 91(7). Pp. 3–15. DOI: 10.18720/MCE.91.1
45. Tusnin, A. Dynamic factors in case of damaging continuous beam supports. Magazine of Civil Engineering. 2018. 78(2). Pp. 47–64. DOI: 10.18720/MCE.78.4

Contacts:

Anatoly Alekseytsev, aalexw@mail.ru